

## Accelerator test of an imaging calorimeter

M. J. Christl<sup>1</sup>, J. H. Adams<sup>1</sup>, R. W. Binns<sup>2</sup>, J. H. Derrickson<sup>1</sup>, W. F. Fountain<sup>1</sup>, L. W. Howell<sup>1</sup>, J. C. Gregory<sup>3</sup>, P. L. Hink<sup>2a</sup>, M. H. Israel<sup>2</sup>, R. M. Kippen<sup>3</sup>, J. Lee<sup>1a</sup>, T. A. Parnell<sup>3</sup>, G. N. Pendleton<sup>3a</sup>, Y. Takahashi<sup>3</sup>, and J. W. Watts<sup>1</sup>

<sup>1</sup>NASA/Marshall Space Flight Center, AL 35812

<sup>2</sup>Washington University, St. Louis, MO 63130

<sup>3</sup>University of Alabama in Huntsville, Huntsville, AL 35899

<sup>a</sup>Former affiliation

**Abstract.** The Imaging Calorimeter for ACCESS (ICA) utilizes a thin sampling calorimeter concept for direct measurements of high-energy cosmic rays. The ICA design uses arrays of small scintillating fibers to measure the energy and trajectory of the produced cascades. A test instrument has been developed to study the performance of this concept at accelerator energies and for comparison with simulations. Two test exposures have been completed using a CERN test beam. Some results from the accelerator tests are presented.

---

of lead or tungsten plates interspersed with x-y planes of thin (0.5mm) square scintillating fibers. Calorimeter depths from 25 to 60 radiation lengths were studied. Performance based trades were made using the resources available for ISS payloads. An ICA prototype test instrument was developed by the collaborators and exposed at CERN in June 1999 and August 2000 to study instrument characteristics and compare with Monte Carlo simulations. A description of the test instrument and current results are presented here and in a companion paper at this conference.

### 1 Introduction

The Advanced Cosmic-Ray Composition Experiment on the International Space Station (ACCESS) is an experiment concept to make direct measurements of the elemental composition and spectra of protons through iron up to the “Knee” (1000 TeV) in the all particle spectrum. The *Baseline* instrument consists of 3 separate detectors: a charge detector, a transition radiation detector and a calorimeter. An ISS accommodation study for the *Baseline* ACCESS has been completed (Wefel99) and several instrument concepts and techniques have been studied (ACCESS00). One of the calorimeter concepts is the Imaging Calorimeter for ACCESS (ICA) that is based on a thin sampling-calorimeter with high-resolution imaging. The starting-point configuration for the ICA concept included separate target and calorimeter modules and an auxiliary charge detector. The targets studied include high and low “Z” materials that varied in thickness from 0-1 proton mean free path ( $\lambda_p$ ). The calorimeter comprises layers

### 2 ICA Accelerator Test

The accelerator test instrument is based on the ICA concept of a thin sampling calorimeter (Figure 1). The active cross section of the instrument is  $13 \times 13 \text{cm}^2$  but the depth can vary depending on the test configuration. The calorimeter has 20 absorber layers, 4.2mm thick lead plates (0.75 rl), and X,Y layer pairs of 0.5mm square scintillating fibers. Each lead plate is mounted in a frame with an orthogonal pair of fiber layers attached to the back. The frames are mounted inside a structure that allow each plane of the calorimeter to be positioned or rotated. Small 1mm stand-offs are used to keep the plates parallel. A thin aluminum foil between each pair of orthogonal fiber layers isolates the scintillation signals. For the target, graphite blocks (0-1 $\lambda_p$ ) are located in front of the calorimeter. For some of the exposures the target was partially instrumented with 4 scintillator paddles made of 1mm scintillating fibers. A light tight shell surrounded the entire instrument.

---

Correspondence to: M. Christl  
[mark.Christl@msfc.nasa.gov](mailto:mark.Christl@msfc.nasa.gov)

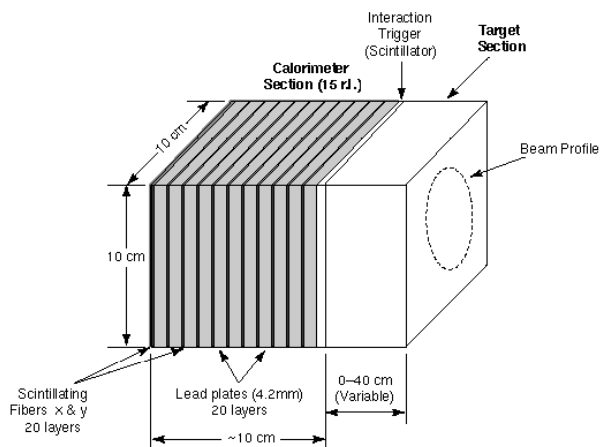


**Figure 1.** ICA Test Instrument Concept

The fiber scintillation signals were measured with 24 photo-multiplier tubes (PMT: 20 calorimeter and 4 target) and an image-intensified CCD system (II-CCD). The Y fibers were grouped by layer and coupled to separate PMTs. In the calorimeter, the opposite end of the Y fibers is formatted onto an II-CCD. The X fibers are formatted onto the same II-CCD input. The CERN beam trigger was obtained from an upstream scintillator that roughly defines the geometry of the beam. An event trigger was generated using the beam trigger, but, for some of the runs an internal calorimeter trigger was included in the trigger logic. For each event the anode and one dynode signal per tube were digitized. Between beam spills pedestal data was automatically acquired. A sample of event images were acquired with the II-CCD for the various configurations to study the imaging aspects of the instrument. The data system included removable disks for data storage, a communication interface to send and receive commands from the instrument and samples of data for online analysis.

The instrument was exposed at the H2 test beam at CERN. This beamline provided Protons and electrons at several energies: 50, 150 & 250 GeV for electrons and 250, 350 & 375 GeV for protons. Exposures were made with several different target thicknesses and with different incident beam angles ranging from 4 to 42 degrees. Specific runs were made for calibration and for studying the performance of the scintillating fibers. Additional details concerning the instrument, performance of the readout systems and fibers can be found in a companion paper.

### 3 Energy Measurements

The principal performance parameters of a calorimeter are the energy response and resolution ( $\rho$ ). The resolution is defined as the root-mean-square of the response distribution divided by its mean. For comparison between simulation and experiment a  $\sigma$  value is usually derived from fitting data to a normal distribution.

The two techniques used to estimate the primary particle energy are “total deposited energy” ( $\Delta E$ ) and “1-dimensional transition curves” ( $I_{\max}$ ). The former method uses the summed scintillation signals of all fibers as a proxy to the total energy deposited in the calorimeter (i.e. both lead and fibers). For the transition-curve technique the energy-related parameter is the maximum development (intensity) of the particle cascade. For both cases the energy deposited in the ICA fibers is a small fraction ( $\sim 1\%$ ) of the total deposited energy, but fluctuations inherent to this sampling technique are small for the primary energies of interest. The dominant fluctuation for thin calorimeters is related to the neutral pion production of the 1<sup>st</sup> interaction (Wigmans91).

The signal for each layer in the calorimeter was normalized using a special configuration wherein primary protons passed through 3 consecutive fibers. The pulse-height-distribution (PHD) of these 3-MIP signals was well above pedestal. The absolute energy calibration is made using pass-through protons in the central region of the active calorimeter. The detection efficiency of the fiber-PMT combination was 80% and the single photoelectron peak was separate from the pedestal peak. The energy results presented here were derived from the PMT readout system only. Some instrumental corrections remain to be made.

The average energy deposition per layer for protons with 3 different targets and for electrons, all at normal incidence, is shown in Figure 2. The respective PHD's for these runs are shown in Figure 3 and include the non-interacting protons in the lower energy bins. The instrument response to protons is governed by the 1<sup>st</sup> interaction and subsequent electromagnetic cascade. Table 1 lists numerical values of the resolution for several instrument configurations. The resolutions for proton cascades were determined after removing non-interacting protons, which was done by applying a signal threshold on 4 of the calorimeter layers. For electrons, the calorimeter performance was largely the same in all the configurations. Some improvement in the measured electron resolution was obtained for the maximum depth configurations because of the reduction in the energy leaking out the back of the instrument.

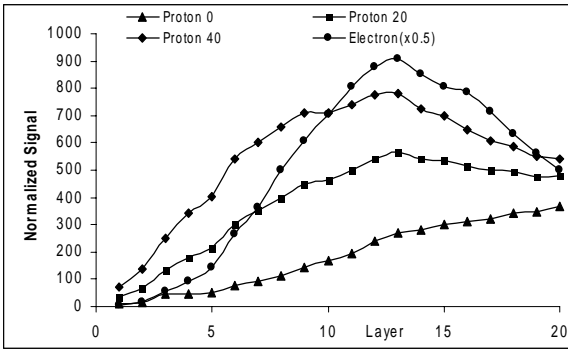


**Figure 2.** Average layer signal in the calorimeter for protons (350GeV) and electrons (150GeV) normally incident. The target thickness for each case is given in the legend in centimeters.

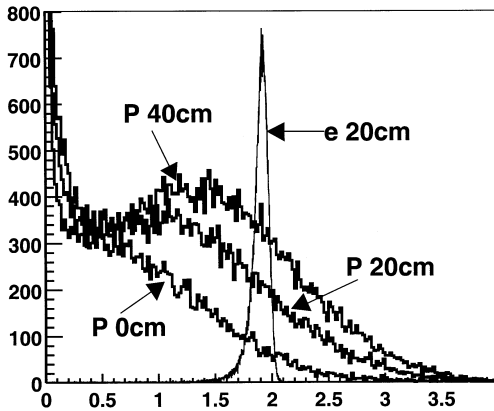


**Figure 3.** Energy Distribution for protons and electron in Figure 2. The energy scale is GeV.

Primary GeV	Target (cm)	Angle (degrees)	$\rho$	$\sigma$
P-350	0	4	66%	0.73
P-350	C - 20	4	55%	0.83
P-350	C - 40	4	52%	0.81
P-350	0	28	54%	
P-350	C - 20	28	55%	
P-350	PE - 40	28	54%	
P-250	C - 40	28	52%	
e-150	C - 20	23	7.2%	0.55

**Table 1.** Energy resolution for several instrument configurations: PE-polyethylene, C-graphite. Sigma is given for a gaussian fit for the PHD's of figure 3.

The second method for estimating the primary energy uses the cascade development in the calorimeter that is largely responsive to the rapid development of the electromagnetic component. The energy deposited in the fibers is used to fit a transition curve for each event. A function similar to Greisen's, originally developed for EAS (Greisen41), is used here. An example of a fitted cascade for a proton primary is shown in Figure 4. The fit parameters, A1-A3, represent the cascade starting depth, depth of shower maximum and max intensity. The PHD of  $I_{max}$  for a proton run is shown in Figure 5 together with the mean response,  $\rho$  and  $\sigma$  for comparison with the  $\Delta E$  method. The example response shown appears to be nearly gaussian.

A direct comparison on an event-by-event bases shows that the relation between  $\Delta E$  and  $I_{max}$  techniques is accurate over the energy distributions measured in the test (Figure 6). However, the fit parameters determined in the  $I_{max}$  technique allow further classification of the cascades such as cascades that are initiated deep in the calorimeter.

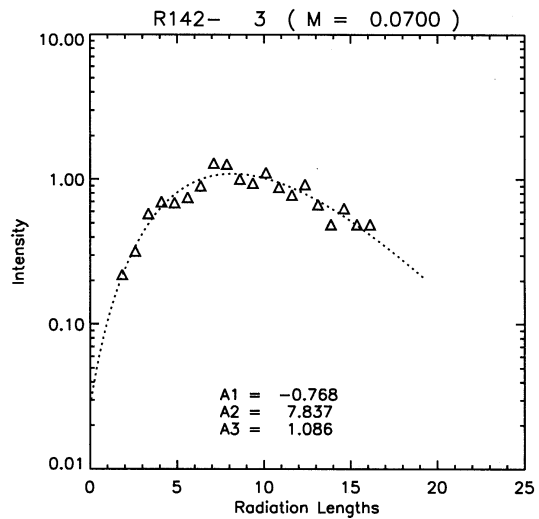


**Figure 4.** Transition curve fitted for single proton.

#### 4 Trajectory Reconstruction

The event trajectory was determined from event images provided by the II-CCD that viewed the 20 X-Y fiber layers in the calorimeter. An image mask was developed that identified each CCD pixel in the image (u,v) with a fiber layer and number (X or Y & Z). The event location (X or Y) at each fiber layer depth in the calorimeter was determined using 3 different methods: position of the maximum single fiber signal, weighted average position and core position. A linear fit to these positions was then used to define the trajectory in the calorimeter and project back to the entrance point in front of the target. The accuracy of the trajectory is defined as the dispersion

of the distribution of all events in the run. This analysis has been completed for normal incidence events and resulted in a position resolution of 1.0 & 1.5 cm for electrons and protons respectively at the top of the target (target thickness of 20cm). All three techniques show similar results at this energy.

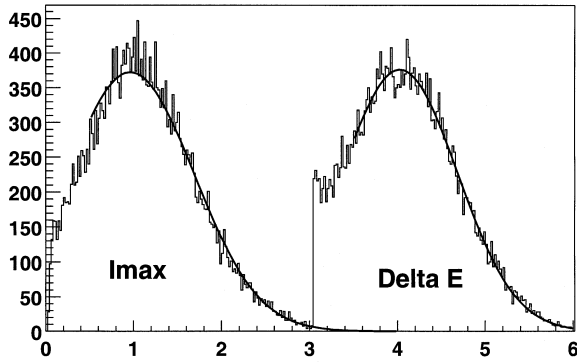


**Figure 5.** PHD of Imax and  $\Delta E$  for protons.  $\rho=52\%$   $\sigma=.69$  for Imax and  $\rho=54\%$   $\sigma=0.66$  for  $\Delta E$ .

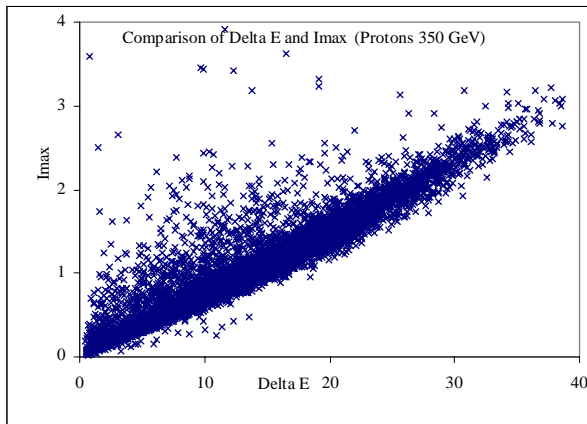


**Figure 6.** Comparison of Imax and  $\Delta E$  for protons at 350 GeV.

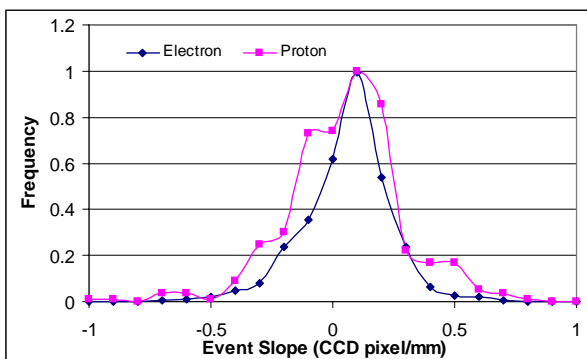


**Figure 7.** Trajectory reconstruction distribution for electrons and protons.

## 5 Simulations

A large simulation effort was completed for the ICA Study using GEANT-Fluka (Parnell01). The test instrument performance is consistent with those simulation results for low energy primary particles. Preliminary simulations have been completed for the test instrument case and appear to support the results presented here. A more detailed comparison of the data and simulated performance will be presented at the conference.

## 6 Conclusions

The shapes of the PHD for protons are well described as gaussian and no high-energy tail was detected in this test. Energy measurements using Imax produce results consistent with the  $\Delta E$  technique for proton and electron primary particles. The Imax technique improves the precision with which a data set can be defined, is more uniform in response for different interaction depths and reduces the required instrument depth.

The fine imaging aspect of the test instrument provided tight pointing accuracy for event trajectory reconstruction. The trajectory accuracy was approximately the beam-spot size ( $\sim 1$ cm). The uncertainty of the trajectory in the calorimeter results in a error when extrapolated to the front of the target of 1cm for electrons and 1.5cm for protons. This result agrees with the simulations completed for the ICA study.

Simulations also show that the  $\Delta E$  resolution remains constant for higher primary energies while the Imax resolution improves with energy. Similarly, the simulations show that the point back accuracy improves with energy.

## 7 References

- (ACCESS00)<http://www701.gsfc.nasa.gov/access/access.htm>  
 (WEFEL99)J. Wefel and T. Wilson, "Advanced Cosmic-Ray Composition Experiment for Space Station", NASA TP-1999-209202 (1999)  
 (Wigmans91) R. Wigmans, Annu. Rev. Nucl. Part. Sci., **41**, 133-185,(1991)  
 (Greisen41)B Rossi and K. Greisen, Rev. Mod. Phys., **13**,240 (1941)  
 (Parnell01)[http://access.phys.psu.edu/frames/home\\_frame.html](http://access.phys.psu.edu/frames/home_frame.html)